P. PANEK*,#

THE INFLUENCE OF THE BASE MATERIAL PARAMETERS ON QUANTUM AND PHOTOCONVERSION EFFICIENCY OF THE Si SOLAR CELLS

The influence of a p-type Si with different resistivity, charge carrier lifetime and emitter dopant impurities concentration on the crystalline silicon solar cells parameters were analyzed and experimentally checked. The findings were determined by quasi-steady-state photoconductance, current-voltage and spectral response methods. The study was accompanied by solar device simulation using a numerical PC1D program. The highest photoconversion efficiency of 15.13 % was obtained for the moncrystalline (Cz-Si) solar cell with a base resistivity of 1.8 Ωcm and an effective charge carrier lifetime of 22.9 μs. The results clearly confirmed the importance concerning the dopant level in a Si base material in relation to open circuit voltage and short circuit current possible to obtain from the solar cell. Reduction of a base material resistivtiy leads to a lower value of an effective charge carrier lifetime and photoconversion efficiency both for Cz-Si and multicrystalline (mc-Si) solar cells. The experimental results and calculation showed, that in the case of a solar cell produced on the basis of crystalline silicon, the most important spectral range for an efficiency of a cell is covering a wavelength range of $587 \div 838$ nm.

Keywords: silicon solar cell, dopant level, charge carrier lifetime.

1. Introduction

The monocrystalline and multicrystalline silicon solar cells are covering over 80 % of photovoltaics (PV) market, while thin film technology is achieving 15 % of production. Compared to the others mass manufactured single junction solar cells, the cells based on crystalline silicon are characterized by the highest efficiency, reaching more than 25 % [1]. In industry, efficiency of the crystalline Si cells claim from manufacturers normally lies between 15 % and 20 %. The performance of solar cell firstly depends on the electronic properties of the silicon, which is a result of dopant impurities as boron or phosphorus added to the molten silicon to change it into an n-type or p-type Si [2]. The dependence of the charge carrier lifetime (τ), or the proportional diffusion length from the doping concentration to Si, is one of the basic issues in the thick-layered technology of Si based solar cell production. The carrier lifetime of a material is defined as the average time for recombination to occur after electron-hole generation [3]. For silicon applied in photovoltaics industry, this takes typically from a few to several microseconds. In this material, the most important recombination losses occur through crystallographic defects and impurities that create energy levels within the band gap and exhibit strongly dependence on the doping density in an emitter and bulk material [4]. Knowledge of the Si net doping density and subsequently, the resistivity (ρ), is important in the optimization of the fabrication process and the explanation of solar cell performance [4]. There are a few important methods for determining the minority carrier lifetime in crystalline silicon material for photovoltaic application [5].

Silicon solar cells are mostly produced on the basis of the p-type silicon with the acceptor concentration (N_A) equaling 1.513×10^{16} atom/cm^3, which corresponds to the base material resistivity of 1 Ωcm. For lower N_A value, one can also obtain a lower cell voltage, and for the N_A value of the order of 10^{17} atom/cm^3 and more, a drop of τ occurs, which is mainly caused by the Auger recombination. This implies a drop of both short circuit current (I_{sc}) and open circuit voltage (V_{oc}) [6].

The sheet resistance (R_{sheet}) of the emitter is another essential parameter, combined with dopant impurities, which determines the emitter saturation current density, the quantum efficiency and the contact resistance properties. The donor doped emitter of the n-type at the depth of about 0.4 μm is gradient in character, with the doping concentration in the near surface area of $\sim 10^{20} \div 10^{22}$ atom/cm^3. The sheet resistance of this area, for a typical cell, is at the level of $40 \div 60$ $\Omega/\square$, which does not cause problems in the creation of an ohmic contact with a low resistivity ~ 3 mΩcm^2, between this area and the front electrode. For the decreasing value of R_{sheet} the cell will have a lower I_{sc} value, and for R_{sheet} at the level of $60 \div 120$ $\Omega/\square$ technological problems occur very often, which are connected with the proper metallization of the front electrode contact.

This work presents a laboratory low cost screen-printed process that yields final solar cells on Cz-Si and mc-Si substrates with different resistivity, lifetime of carriers and emitter dopant impurities concentration. Due to the fact, that one cannot directly compare the results between cells based on Cz-Si and mc-Si, the material used in this work is characterized by two values of resistivity and lifetime for each type of Si (Table 1).

* INSTITUTE OF METALLURGY AND MATERIAL SCIENCE, POLISH ACADEMY OF SCIENCES, 25 REYMONTA STR., 30-059 KRAKOW, POLAND

Corresponding author: pan-kozy@wp.pl

2. Theoretical calculation

The PC1D computer program [7], which solves the fully coupled nonlinear equations for quasi one dimensional transport of electrons and holes in crystalline Si device, was applied to calculate the correlation between resistivity of a bulk p-type Si material and main output I-V electrical parameters of a solar cell [8]. The constant parameters used for calculation of the correlation mentioned above were: device area - 100 cm^2, cell thickness - 170 µm, exterior front reflectance in a wavelength range of 400 ÷ 1100 nm - 10 %, minority carrier lifetime (τ) - 15 µs, Gaussian profile emitter with peak doping of 1.445 x 10^{20} cm^{-3}, junction depth - 0.317 µm, emitter sheet resistance - 60 $\Omega/\square$, front surface recombination velocity - 1000 cm/s and back surface recombination velocity - 10000 cm/s. The calculated dependence of the resistivity on short circuit current and open circuit voltage in the range of 0.3 ÷ 5.0 Ωcm is shown in Fig. 1. The material characterized by this range of a resistivity is most often used by the R&D and PV industry sectors.
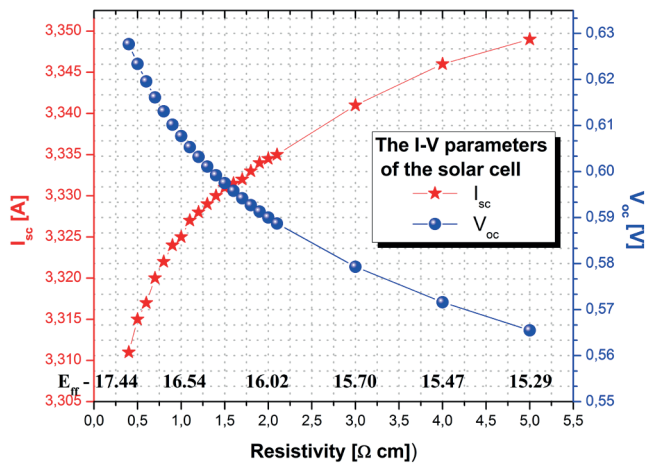

Fig. 1. The calculated variation of the short circuit current and open circuit voltage as a function of the base material resistivity. The corresponding solar cell photoconversion efficiencies E$_{ff}$ are enclosed in the form of the calculated values

The graph indicates that the short circuit current is inversely proportional to the doping concentration in the base. This should be as high as possible, however, the lifetime of minority carriers decreases with higher doping [6]. If the doping level exceeds about 1 x 10^{17} atom/cm^3, the Auger recombination mechanism becomes dominant even in good quality silicon. Hence, the carrier lifetimes in the emitters which posses higher doping level than base material are usually limited by Auger recombination [9]. The effect associated with the amount of dopant in Si can be detected, among others techniques, by external quantum efficiency (EQE) measurements [10]. The influence of base Si parameters ρ and τ on a EQE for two selected values were used for numerical calculations and results are graphically presented in Fig. 2.

The calculations concerning the main impact of the resistivity and lifetime on the external quantum efficiency of the cells showed that a significant influence on the reduction of EQE in a wavelength range of 600 ÷ 1100 nm exhibits

a low lifetime of charge carriers, not the value of a material resistivity. On the other hand, fabrication of the Si base material having a lifetime of more than several tens of microseconds and a resistivity about 0.1 Ωcm, which means for p-type Si the acceptor doping level of 10^{17} atom/cm^3, is not an easy process. Anyway, the base doping can be higher than for traditional range of 0.5 ÷ 1.5 Ωcm, used for cell with a thickness of around 200 µm, since the reduction in diffusion length with increasing base doping is tolerable due to the smaller cell thickness. For solar cells fabricated on Si with base resistivity under 0.5 Ωcm it is also necessary to include band gap narrowing [11].

As the conclusion from the numerical calculations, it is safe to say that to produce Si solar cell one should apply the material with the lowest possible resistivity values but also characterized by the highest value of the lifetime of charge carriers.
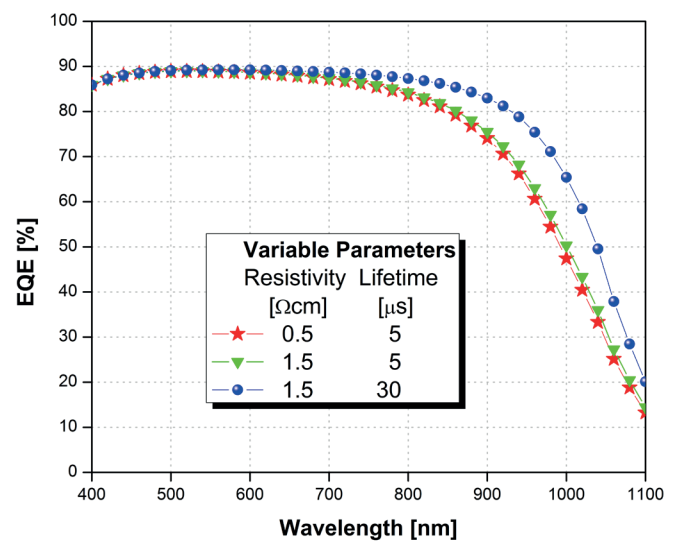

Fig. 2. Calculated by PC1D modeled impact of the resistivity and lifetime on external quantum efficiency for Si based solar cell.

3. Experimental procedure

The samples in the form of symmetrical structures for the measurement of a lifetime and final solar cells were prepared on 5 x 5 cm multicrystalline and (100) oriented monocrystalline silicon wafers, textured on both surfaces. The wafers, after defected layers removing and texturization process were 170 µm thick. A detailed list of parameters for materials used in this work is summarized in Table 1.

Minority carrier lifetime of the bare wafers after defected layer removing was first measured, followed by determination after each fabrication step prior to metallization and the results are shown in Table 1. For a base material characterization, a passivation process at 800 ºC in dry oxide for 10 min. was curried out. The minority carrier lifetime was analyzed by quasi-steady-state photoconductance technique. A WTC-120 instrument from Sinton Consulting was applied and the lifetime was recorded at an injection level of excess charge carrier concentration $\Delta n = 5$ x 10^{14} cm^{-3}. Standard industrial solar cells operate in the range of $\Delta n = 1$ x 10^{13} cm^{-3} ÷ 1 x 10^{15} cm^{-3}, while high

TABLE 1

The main Si material parameters and effective lifetime after defected layer removal (τ_{eff-1}), and next, after diffusion (τ_{eff-2}), and passivation (τ_{eff-3}), process

Solar cell	Resistivity [Ωcm]	R_{sheet} [$\Omega/\square$]	Lifetime τ_{eff-1} [μs]	Lifetime τ_{eff-2} [μs]	Lifetime τ_{eff-3} [μs]
Cz-Si-1	0.9	60	6.6	9.8	10.9
Cz-Si-2	1.8	45	14.7	18.9	22.7
Cz-Si-3	1.8	60	15.0	20.0	22.9
mc-Si-1	0.7	60	3.0	3.8	4.9
mc-Si-2	1.4	45	6.6	8.0	10.8
mc-Si-3	1.4	60	6.4	8.9	11.4

efficiency cells can reach $\Delta n = 1 \times 10^{16}$ cm^{-3} under operating conditions [5]. The lifetime, in the case of the experimental measurements reported in this paper, must be considered as effective lifetime (τ_{eff}), which incorporates all the bulk and surface recombination processes.

The data in Table 1 presents, that a maximum effective lifetime of 22.9 μs has been measured for lightly doped Cz-Si-3 material with resistivity of 1.8 Ωcm. Table 1 shows, that after each technology step, the mc-Si material possesses much worse τ_{eff} than value for Cz-Si material. The measured lifetime is correlated to the resistivity of the substrate, with lower ρ being accompanied by lower τ_{eff}. Each of the high temperature process, that is phosphorus diffusion and oxidation technique, was found to have a very strong impact on the effective carrier lifetime. The improvement is attributed partly to the surface passivation with the oxide layer formed after diffusion process and partly to the gettering of the impurities in silicon wafers during phosphorus diffusion [12]. The minimum of a minority carrier lifetime limit in p-type solar-grade silicon is around 2 μs. A significant increase of a lifetime for base bulk Si material is usually realized as a result of gettering in the temperature range from 1100 to 1200 $^{\circ}$C. Lifetime improvement as a result of the variable temperature process from $3 \div 7$ μs up to 81 μs with gettering was found but such high temperature process is not applied during solar cells fabrication [13]. Presently, a p type Cz-Si with resistivity of 1 Ωcm and lifetimes exceeding 1 ms is available [14].

The diffusion processes were performed at 845 $^{\circ}$C and 860 $^{\circ}$C for 30 min. with phosphorus delivered by a POCl$_3$ liquid source. This yields an emitter with a sheet resistance of 60 and 45 $\Omega/\square$, respectively. The phosphoro-silica glass (PSG) was removed by immersion in a bath of HF:H$_2$O (1:9 vol.) solution for 2 min. The surface passivation for mc-Si solar cells was achieved by the 12 nm thick SiO$_2$ grown at 800 $^{\circ}$C for 10 min. In the case of Cz-Si solar cells, the process was carried out at 840 $^{\circ}$C for the same time. To assure an ARC front layer, the 70 nm thick titanium dioxide layer was deposited by CVD method using (C$_2$H$_5$O)$_4$Ti as a source. The screen printing technique was used with Du Pont PV18A paste for front contact and PV505, PV381(Al) for back contacts. After oven drying at 150 $^{\circ}$C for 10 min, the printed samples were co-fired in III zones IR belt furnace running at belt speed of 200 cm/min at 920 $^{\circ}$C peak temperature in purified natural atmosphere ambient.

4. Solar cells characterization

The solar cells were characterized by the light current-voltage (I-V) measurements at Solar Simulator SS200 AAA class EM Photo Emission Tech., Inc. with Solar Cells I-V Curve Tracer SS I-V CT-02 PV. The data was obtained under AM1.5 global spectrum at 1000 W/m^2 light intensity at temperature of 25 $^{\circ}$C. The reference cell No. 005-2013 was calibrated at Fraunhofer ISE.

The highest efficiency of 15.13 % was obtained for the Cz-Si-3 solar cell with a base resistivity of 1.4 Ωcm and an effective lifetime of 22.9 μs (Table 1). The measured output I-V parameters give lower efficiency for Cz-Si-1 and mc-Si-1 cells with lower effective lifetime (Table 1). According to calculation by PC1D, the cells based on lower resistivity Si

TABLE 2

The I-V parameters of the 25 cm^2 solar cells fabricated by application of the POCl$_3$ solutions as a donor source on p-type, Cz-Si and mc-Si textured wafers

Cell	I_{sc} [A]	V_{oc} [V]	P_m [W]	FF [%]	R_s [mΩ]	R_{sh} [Ω]	E_{ff} [%]
Cz-Si-1	0.813	0.599	0.370	75.9	50.6	93.42	14.81
Cz-Si-2	0.817	0.602	0.378	76.8	51.6	106.80	15.12
Cz-Si-3	0.836	0.600	0.378	75.4	52.6	94.76	15.13
mc-Si-1	0.752	0.593	0.336	75.1	51.0	90.64	13.44
mc-Si-2	0.762	0.596	0.342	75.4	55.0	123.29	13.70
mc-Si-3	0.770	0.597	0.344	74.9	56.4	96.32	13.78

where: I_{sc} - short circuit current, V_{oc} – open circuit voltage, P_m – optimum power point, FF – fill factor, R_s – series resistance, R_{sh} – shunt resistance, E_{ff} – conversion efficiency.

should have the highest voltage (Fig. 1), but the experimental results are contrary to relation of V_{oc} between the Cz-Si-1 and Cz-Si-3 and between the mc-Si-1 and mc-Si-3 solar cells. Comparison of these cells makes sense because of the identical diffusion process and characteristics of their emitters. This V_{oc} effect can be explained by the difference in the effective lifetime, which for the cells with higher V_{oc} is about two times better. The reason is bonded with the lower I_{sc} for mc-Si-1 and Cz-Si-1 cells, which is correlated with V_{oc} by the following relationship [6] [9]:

$$V_{oc} = kT/q \ \ln (I_{sc}/I_o - 1) \tag{1}$$

where: k – Boltzmann constant, T – temperature, q – elementary charge and I_o – dark saturation current.

According to above relation, a high open-circuit voltage is achieved for the solar cell characterized also by a low dark saturation current, which for a base is reduced with $1/N_A$ and large short-circuit current. The reason also lies on the side of Si wafers used in the experimental work, for which the difference in resistivity between Cz-Si-1 and Cz-Si-3 is 0.9 Ωcm and between mc-Si-1 and mc-Si-3 is 0.7 Ωcm (Table 1). This difference implies the change of the cell V_{oc} by only about ~ 10 mV (Fig. 1). The same V_{oc} behavior was observed for mc-Si with base resistivity in a range from 0.5 to 9.0 Ωcm, after gettering process [15]. A characteristic feature of the solar cells mc-Si-2 and Cz-Si-2 with the sheet resistance of 45 Ω/□ is the highest value of FF, which results from greater depth and the value of the emitter dopant and finally the maximum values of shunt resistance for the fabricated cells in each series. The difference in sheet resistance of only 15 Ω/□ does not determine decisively series resistance of the cells, which is between 50.6 ÷ 56.4 mΩ, which indicates the uniformity of the metallization process. The experimental results clearly confirm the importance of the dopant level in Si in relation to short-circuit current which is possible to obtain from the cell, both in the emitter and base region. Minimization of additives cannot be arbitrary and must take into account losses of V_{oc} and R_s.

To evaluate the process of generation and recombination of the charge carriers for fabricated solar cells, the measurements an external quantum efficiency (EQE) of the cells were performed using Yobin Yvon H20 IR monochromator with halogen lamp, working in a wavelength (λ) range of 400 ÷ 1110 nm. The applied beam splitter set up allowed a simultaneously determination of the I_{ph} for Hamamatsu photodiode S2281/5D/1299 and I_{cell} for the investigated solar cell. The reference cell No. 005-2013 for EQE measurements was calibrated at Fraunhofer ISE. The final results are presented in Figs. 3 and 4.

The results presented in Figs. 3 and 4 indicate, that for Si bulk material, both for mc-Si and Cz-Si cells with this same R_{sheet}, lower effective lifetime decreased the EQE especially in a wavelength range of 600 ÷ 1100 nm, due to recombination losses within the base of the solar cells. The experimental dependence of the EQE also confirms the results of a theoretical calculation by PC1D which are shown in Fig. 2. A consequence of the highly doped emitter with lower value

of R_{sheet} (Tab. 1) can be seen in Fig. 3 and 4. The EQE response in a wavelength range of 400 ÷ 600 nm, which reflected the influence of the emitter region, is degraded for both Cz-Si-2 and mc-Si-2 cells.
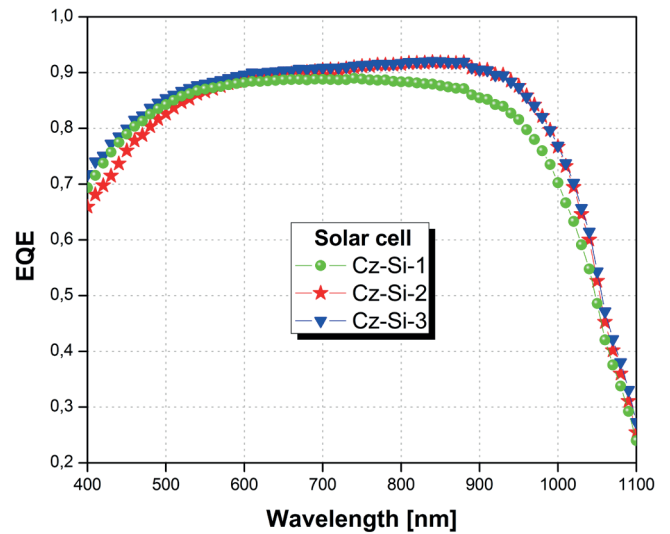

Fig. 3. Comparison of an external quantum efficiency of the Cz-Si solar cells
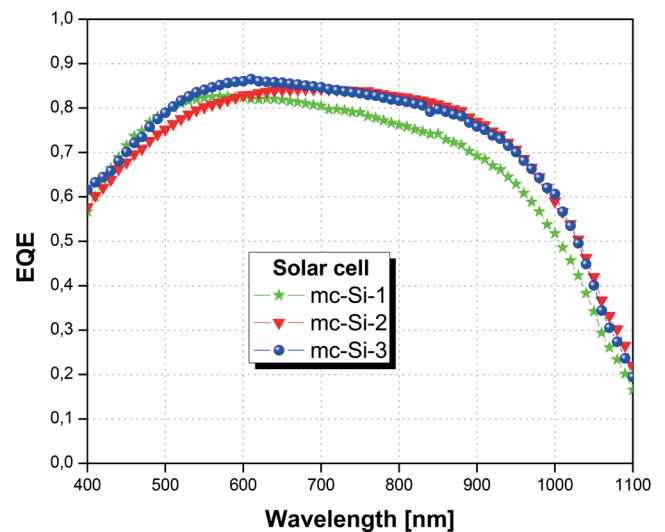

Fig. 4. Comparison of an external quantum efficiency of the mc-Si solar cells

The knowledge of the external quantum efficiency in a given wavelength range of radiation made it possible to directly calculate the density of the short-circuit current ($J_{sc}(\lambda)$) of the cell from the formula (2) and final evaluation of the spectral response of the solar cells [16]:

$$SR(\lambda) = J_{sc}(\lambda)/P_{in}(\lambda) = (q\lambda/hc) \ EQE(\lambda) \tag{2}$$

where: $J_{sc}(\lambda)$ - density of the current from the solar cell for a given wavelength, $P_{in}(\lambda)$ - radiation intensity determined by the foton flux $N_{ph}(\lambda)$ according to formula $P_{in}(\lambda) = (hc/\lambda) N_{ph}(\lambda)$, h – Planck constant, c – speed of light in vacuum.
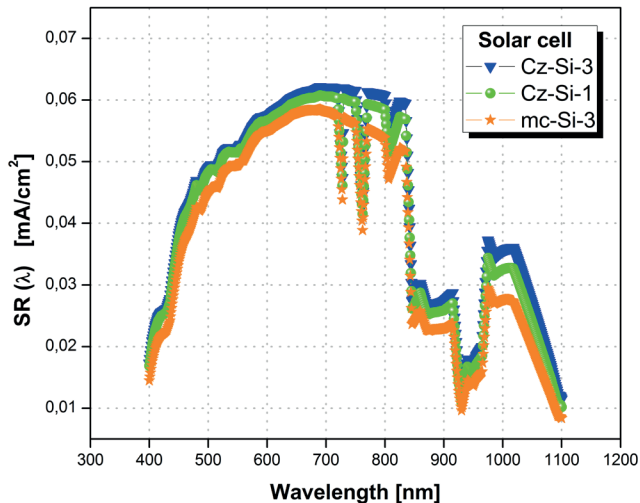
Fig. 5. Spectral response for solar cells with the best value of photoconversion efficiency based on monocrystalline Si – cell Cz-Si-3 and on multicrystalline Si – cell mc-Si-3. For comparison, the SR(λ) characterized the cell Cz-Si-1 on monocrystalline Si with lowest effective lifetime of 10.9 μs is enclosed

The dependence SR(λ) shown in Fig. 5 allows a calculation of the current density for a given wavelength. For example, the cell Cz-Si-3 with the highest photoconversion efficiency of 15.13 % (Table 2), produces 0.0619 mA per square centimeter for a wavelength of 730 nm. Interval with a wavelength between 587 ÷ 838 nm is also the most important spectral range for a operation in the case of a solar cell produced on the basis of crystalline silicon. The effective lifetime of the charge carriers equal to 22.9 μs (Table 1) enables to reach the highest photocurrent for the Cz-Si-3 cell compared to Cz-Si-1 cell with τ_{eff} of 10.9 μs.

For chosen solar cells, the functions SR(λ) was integrated in the range from 400 to 1100 nm and a current density of the cells was calculated. The calculated J_{sc} values for the solar cells denoted as: mc-Si-3, Cz-Si-1, and Cz-Si-3 amounted respectively: 27.70, 29.86 and 30.88 mA/cm². Compared to J_{sc} values obtained by current-voltage characteristics measurements (Table 2), they are lower by 2.38, 2.66 and 2.56 mA/cm², respectively. The source of the above differences is the fact, that the EQE measurement on the Yobin Yvon H20 IR monochromator covering a wavelength range of 400 ÷ 1100 nm (Fig. 5). The second reason is related to the difference between a theoretical dependences of the photon flux used for SR(λ) calculation and real spectrum of the lamp during an I-V measurements.

This consideration has serious consequences for the certified measurements of photovoltaic cells and modules. First, a correct methodology forces a measurement of a SR(λ) dependence, and then, a calculation of the short circuit current I_{sc}. The I_{sc} value is a base for further calibration the I-V set up in terms of the value for a generated photocurrent produced by a measured solar cell in relation to the radiation intensity $P_{in}(\lambda)$. For this reason, a proper measurements of a SR(λ), in the case of the crystalline Si based solar cells, require a monochromator with resolution of 1 nm and covering a wavelength range of 300 ÷ 1200 nm. This broader range under 400 nm wavelength allows also to determine a surface recombination velocity (SRV) of a solar cell.

In order to determine the areas which posses a strongest effect on recombination process within the silicon solar cell, the measurement by light beam induced current (LBIC) method was done. The LBIC maps were performed using the 20 mW diode lasers at light spot resolution of about 10 μm. The map obtained at incident a wavelength of 405 nm is presented in Fig. 6 (a) and at incident a wavelength of 808 nm is presented in Fig. 6 (b). The blue color, on the LBIC maps shown in Fig. 6, represents the high degraded areas for photoconvertion process.
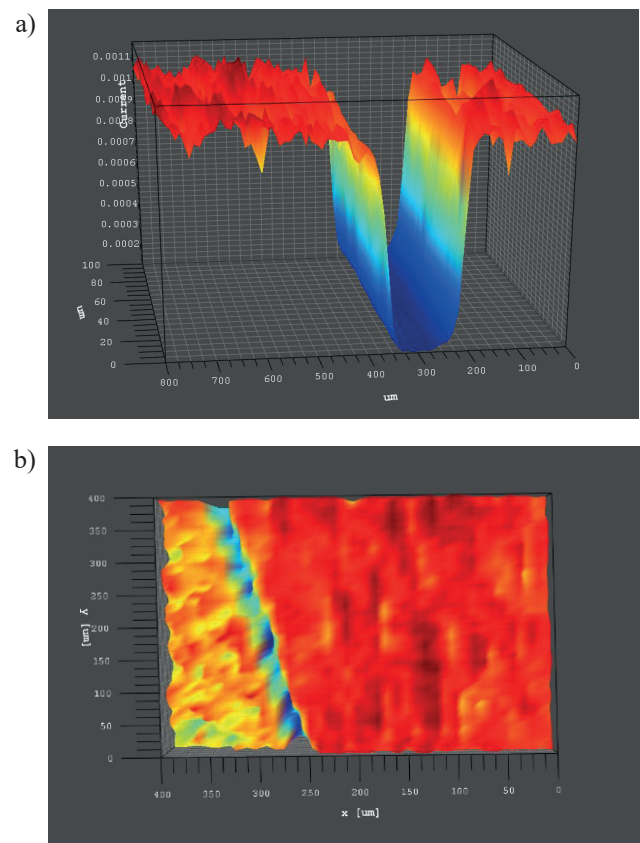
a)

b)

Fig. 6. The LBIC maps of the electrically degraded area under the front silver finer of the (100) oriented Cz-Si solar cell (a), and in the boundary area between two grains of mc-Si solar cell (b).

Presented in Fig. 6(a) the degraded area under the front silver finger of the (100) oriented Cz-Si solar cell is due to a fact, that the Ag precipitates and crystallites are coexisting at the Ag/Si interface, and where only a current transport take place [17]. The LBIC map of the area under the front contact finger also reflects a shading loss. The area where the lifetime of charge carries is reduced, most important in the case of mc-Si, is boundary area between two grains with different crystallographic orientation, shown in Fig. 6(b) as blue non-regular line.

5. Conclusions

Minority carrier effective lifetime of wafers was measured after each step of solar cell fabrication. A significant improvement in lifetime by 5.0 μs was detected after phosphorus

diffusion step. The improvement is attributed to gettering of the impurities in silicon wafers and surface passivation with the oxide layer formed during diffusion process [9]. According to the results of the numerical calculations, the highest photovoltaic conversion efficiency value should reach the solar cell based on Si which is characterized by the combination of the lowest resistivity and the highest value of the charge carrier lifetime. The experimental results confirm only a significant impact of the lifetime on E_{ff}, while the low resistivity values causes a growth of the cell voltage without compensation of I_{sc} which degradation limited the solar cell efficiency.

The EQE results indicated, that for Si bulk material, both for mc-Si and Cz-Si cells with the same emitter, lower effective lifetime decreased the EQE especially in a wavelength range of 600 ÷ 1100 nm, due to recombination losses within the base of the solar cells. The experimental results and calculation showed, that in the case of a solar cell produced on the basis of crystalline silicon, the most important spectral range for an operation covering a wavelength range of 587 ÷ 838 nm.

Despite, the non optimized technology process, especially considering the fact that the SiO_2/TiO_2 layers have been applied instead generally used SiN_x:H layer and a texturization process by KOH chemical treatments, the mc-Si solar cell with efficiency of 13.78 % was fabricated. Under IMMS Photovoltaic Laboratory conditions, with current state of the art technology, with TiO_2 as antireflective coating, it is possible to produce solar cells based on Cz-Si with efficiency of 15.13 %.

Acknowledgement

REFERENCES

[1] M. A. Green, K. Emery, Y. Hishikawa, W. Warta, E.D. Dunlop, Prog. in Photov.: Research and Applic. **24**, 905-913 (2006).

[2] V.V. Tyagi, N.A.A. Rahim, N.A. Rahim, J.A.L. Selvaraj, Renewable and Sustainable Energy Reviews **20**, 443–461 (2013).

[3] S.R. Wenham, M.A. Green, M.E. Watt, R.P. Corkish, A.B. Sproul, Applied Photovoltaics, Earthscan, New York, USA, 2011.

[4] T. Markvart, L. Castañer, Solar Cells – Materials, Manufacture and Operation, Elsevier, Amsterdam, Netherlands, 2005.

[5] P. Rosenits, Photov. Internat. **4**, 35-41 (2010).

[6] A. Goetzberger, J. Knobloch, B. Voss, Crystalline Silicon Solar Cell, John Wiley & Sons, Chichester, England, 1998.

[7] https://www.engineering.unsw.edu.au/energy-engineering/pc-1d-software.html

[8] P.A. Basore, IEEE Trans. on Electron Devices **37**, 337-343 (1990).

[9] A.G. Aberle, Crystalline silicon solar cells, Bloxham and Chambers Ltd., Rhodes, Australia, 1999.

[10] S.M. Sze, K.K. Ng, Physics of Semiconductor Devices, John Wiley & Sons, Hoboken, USA, 2007.

[11] S.W. Glunz, J. Dicker, P.P. Altermatt, Proc. of the 17th Europ. Photov. Sol. Ener. Conf., Munich, Germany, 1391 – 1395 (2001).

[12] S.K. Dhungel, J. Yoo, K. Kim, S. Ghosh, S. Jung, J. Yi, Mater. Science and Engin. (B) **134**, 187-290 (2006).

[13] V. Osinniy, A.N. Larsen a, E.H. Dahl, E. Enebakk, A.K. Søiland, R. Tronstad, Y.Safir, Solar Ener. Mater. & Solar Cells, **101**, 123–130 (2012).

[14] D.C. Walter, B. Lim, K. Bothe, R. Falster, V. V. Voronkov, J. Schmidt, Solar Ener. Mater. & Solar Cells **131**, 51–57 (2014).

[15] O. Schultz, S. W. Glunz, S. Riepe, G. W. Willeke, Prog. in Photov.: Research and Applic. **14**, 711-719 (2006).

[16] N.A. Arora, J.R. Hauser, IEEE Trans. on Electron Devices, **ED-34**, 430-434 (1984).

[17] J. Qin, W. Zhang, S. Bai, Z. Liu, Appl. Surf. Science **376**, 52-61 (2016).